Journal of The Electrochemical Society, **156** (6) J138-J142 (2009)
0013-4651/2009/156(6)/J138/5/$25.00 © The Electrochemical Society

Emission Band Change of $(Sr_{1-x}M_x)_3SiO_5:Eu^{2+}$ (M = Ca, Ba) Phosphor for White Light Sources Using Blue/Near-Ultraviolet LEDs

Ho Seong Jang,[a] Yu-Ho Won,[b] Sivakumar Vaidyanathan, Dong Hyuk Kim, and Duk Young Jeon[*,z]

Department of Materials Science and Engineering, Korea Advanced Institute of Science and Technology, Yuseong-gu, Daejeon 305-701, Korea

The luminescence properties of orange-yellow-emitting Eu^{2+}-activated Sr_3SiO_5 were optimized for application to blue/near ultraviolet (n-UV) light-emitting diodes (LEDs). $Sr_{2.97}SiO_5:Eu^{2+}_{0.03}$ showed strong orange-yellow emission peaking at ~580 nm under blue and n-UV light of 450 and 405 nm, respectively, and the effects of Ca and Ba substitutions into Sr^{2+} sites on the emission band change were investigated. For the substitution of Ca, $Ca_3SiO_5:Eu^{2+}$ showed no orange-yellow emission under blue light due to the different crystal structures of Ca_3SiO_5 (monoclinic) and Sr_3SiO_5 (tetragonal). The redshift and blueshift of the emission band of $(Sr_{1-x}Ba_x)_3SiO_5:Eu^{2+}$ were explained by the competition between crystal field effect and Nephelauxetic effect. The 460 nm-emitting blue LED-pumped white LED with $Sr_3SiO_5:Eu^{2+}$ or a mixture of $Sr_3SiO_5:Eu^{2+}$ and green phosphor ($Ba_2SiO_4:Eu^{2+}$) were fabricated and they showed color coordinates of (0.343, 0.281) and (0.349, 0.339), respectively.
 [DOI: 10.1149/1.3106042]

Manuscript submitted September 8, 2008; revised manuscript received February 9, 2009. Published April 6, 2009.

Next-generation white light sources are generated from a combination of blue light-emitting diodes (LEDs) and a yellow-emitting $Y_3Al_5O_{12}:Ce^{3+}$ (YAG:Ce) phosphor.[1] White light sources such as phosphor-converted white LEDs have many advantages such as high brightness, low power consumption, and long lifetime (~100,000 h).[2-5] The yellow-emitting YAG:Ce has a strong excitation band in the 450–470 nm region which corresponds to the emission band of blue LEDs and shows strong broad yellow emission.[6,7] Therefore, the YAG:Ce is appropriate for application to blue LED-pumped white LEDs and has already been commercialized. However, because the emission intensity of YAG:Ce is weak in the red spectral region, the color-rendering property of YAG:Ce-based white LEDs is poor.[3,8,9] Besides use as a yellow-emitting YAG:Ce phosphor, Park et al. reported that Eu^{2+}-activated Sr_3SiO_5 can be a good candidate for white light source applications using blue LEDs.[10] When a $Sr_3SiO_5:Eu^{2+}$ phosphor is coated on a blue LED chip, the phosphor shows broad orange-yellow emission peaking at about 580 nm. The white LED combining a blue LED with an orange-yellow-emitting $Sr_3SiO_5:Eu^{2+}$ phosphor shows a low color-rendering index of below 70, which is not acceptable to general illumination. This is due to deficiency of emission intensity in the green spectral region.[10] If the emission band shifts to a shorter wavelength, the emission intensity in the green spectral region can be enhanced. The excited electronic configuration of Eu^{2+} ion is $4f^65d^1$, and the emission is attributed to the electronic transition of $4f^65d^1 \rightarrow 4f^7$.[11] As a consequence, the Eu^{2+} shows a broad emission band which strongly depends on the chemical nature of the host lattice surrounding the Eu^{2+} ions present in the host lattice.[12] The 5d orbital of Eu^{2+} strongly interacts with neighborhood ligand ions, and the position of the degenerate 5d band depends on the crystal field strength. Through the change of the host lattice, the luminescence of Eu^{2+} can be adjusted with different crystal field splitting of the 5d band. The emission intensity of $Sr_3SiO_5:Eu^{2+}$ could be enhanced in the green or red spectral region via an emission band shift to the green or red region due to host lattice modification. Because the second emission band in blue LED-pumped white LEDs which is attributed to the phosphor influences the color temperature, the Commission Internationale de l'Eclairage (CIE) color coordinates, and color rendering of the white LEDs, the optical properties of white LEDs can be improved by control of the luminescence of the phosphor.[13]

In the present study, a series of M^{2+}-substituted compositions $(Sr_{1-x}M_x)_3SiO_5:Eu^{2+}$ (M = Ca, Ba) have been synthesized in order to manipulate the emission. A detailed investigation of powder X-ray diffraction (XRD) and photoluminescence (PL) has been carried out. In addition, white LEDs have been fabricated by combining the presently studied phosphor with blue or near ultraviolet (n-UV) LEDs and their optical properties have been investigated.

Experimental

To synthesize $Sr_3SiO_5:Eu^{2+}$ phosphor, high-purity strontium carbonate ($SrCO_3$, Aldrich 99.995%), silicon oxide (SiO_2, Kojundo Chemicals 99.9%), and europium oxide (Eu_2O_3, Aldrich 99.99%) were used as raw materials. They were mixed thoroughly by using ethanol as a solvent for mixing. Raw materials were fired at temperatures above 1200°C in a reducing atmosphere. The synthesized phosphors were orange-yellow in body color, which confirms the presence of Eu^{2+} ions in Sr^{2+} sites. The phase identification of the prepared samples was determined by XRD measurement using a $\theta/2\theta$ goniometer [Rigaku, D/max-IIIC (3 kW) with Cu Kα radiation (λ = 1.5418 Å) at 40 kV and 45 mA]. The scan rate was 3°/min and covered the range between 15 and 80°. In order to investigate luminescent properties of the Eu^{2+}-activated silicate phosphor samples, PL was measured using a Darsa PRO5100 PL system (PSI Trading Co., Ltd., Korea) with a xenon lamp (500 W). Measurements were done at λ_{ex} of 450 nm. PL excitation (PLE) spectra were obtained by using a Perkin-Elmer LS-50 luminescence spectrometer. The morphology and particle size of the samples were observed by scanning electron microscopy (SEM) (Philips XL30SFEG). Electroluminescence (EL) spectra of the fabricated white LEDs were measured with a monochromator in the PL system at 20 mA.

Results and Discussion

In order to optimize the PL property of a $Sr_3SiO_5:Eu^{2+}$ phosphor, firing temperature was the first variable considered. The $Sr_3SiO_5:Eu^{2+}$ phosphor was synthesized at various temperatures ranging from 1200 to 1350°C. Figure 1 shows the PL spectra of $Sr_3SiO_5:Eu^{2+}$ phosphor samples with various firing temperatures under 450 nm excitation. $Sr_3SiO_5:Eu^{2+}$ showed a broad orange-yellow emission band with a maximum peak wavelength at about 580 nm. The broad orange-yellow emission of the phosphor is attributed to the $4f^65d^1 \rightarrow 4f^7$ transition of the Eu^{2+} ion.[11] The energy level of

* Electrochemical Society Active Member.
[a] Present address: Department of Chemistry, Purdue University, West Lafayette, Indiana 47907, USA.
[b] Present address: School of Materials Engineering, Purdue University, West Lafayette, Indiana 47907, USA.
[z] E-mail: dyj@kaist.ac.kr

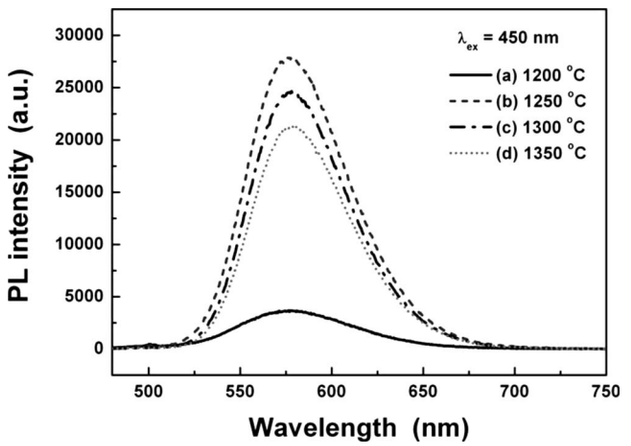

Figure 1. PL spectra of $Sr_3SiO_5:Eu^{2+}$ phosphor samples synthesized at various temperatures under 450 nm excitation: (a) 1200, (b) 1250, (c) 1300, and (d) 1350°C.

the $5d^1$ configuration is split to form a broad band by the crystal field. The energy difference between the lowest excited 5d band and ground $^8S_{7/2}$ state is about 22,000 cm^{-1}. This energy corresponds to a blue light wavelength so that $Sr_3SiO_5:Eu^{2+}$ phosphor absorbs blue light and emits orange-yellow light. Therefore, it can be applied to white light sources pumped by blue LEDs.

As seen in the XRD patterns in Fig. 2, when firing temperature was higher than 1200°C, a pure tetragonal phase was formed. When heat-treatment was carried out at 1200°C, impurity phases coexisted with the tetragonal Sr_3SiO_5 phase. When firing temperature was increased, thermal energy was enough to help raw materials diffuse into one another and helped Eu^{2+} ions to substitute Sr^{2+} sites. Therefore, temperatures above 1200°C reduced impurities and increased crystallinity. Although the impurities were reduced and diffraction intensity was high at temperatures above 1200°C, PL intensity did not increase as a function of firing temperature. As firing temperature was increased, particle size became large and agglomeration among particles increased as shown in the SEM images of Fig. 3. When the firing temperature was larger than 1250°C, the agglomeration was prominent. Beyond 1300°C, the agglomeration appeared to be a main factor affecting the decrease of PL intensity of Eu^{2+} emission in Sr_3SiO_5.

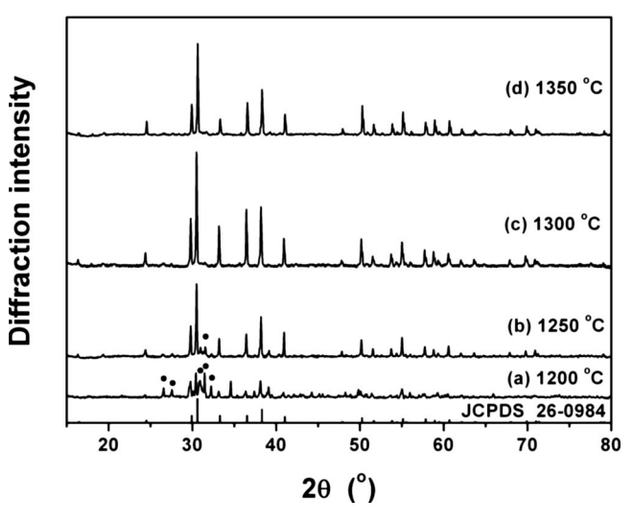

Figure 2. XRD patterns of $Sr_3SiO_5:Eu^{2+}$ synthesized at various firing temperatures: (a) 1200, (b) 1250, (c) 1300, and (d) 1350°C. (●) Impurity phase.

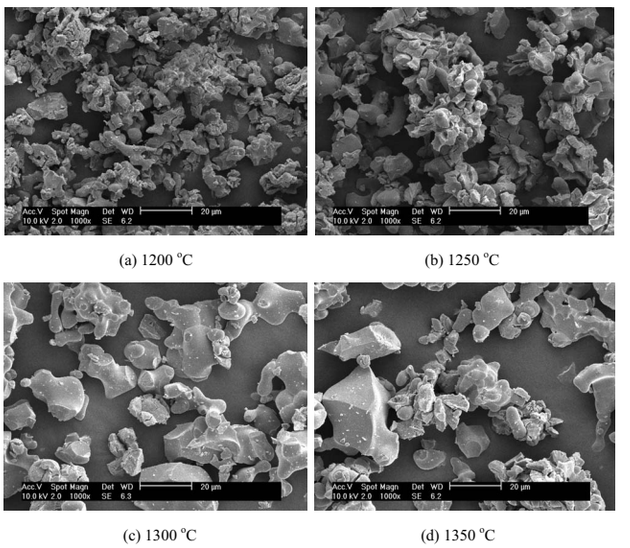

Figure 3. SEM images of $Sr_3SiO_5:Eu^{2+}$ phosphors synthesized at (a) 1200, (b) 1250, (c) 1300, and (d) 1350°C.

Figure 4 shows the maximum PL intensity and the dominant wavelength of $(Sr_{1-x}Eu_x)_3SiO_5$ phosphor (x = 0.005, 0.01, 0.015, 0.02, and 0.03). In this experiment, the optimized Eu^{2+} concentration was 1 mol %. When the concentration of Eu^{2+} ions was over 1 mol %, concentration quenching occurred and PL intensity decreased with increasing Eu^{2+} ions. Emission wavelength as well as emission intensity were changed by varying the amount of Eu^{2+} ions. As the amount of Eu^{2+} ions in the host lattice was increased, the emission wavelength shifted slightly to a longer wavelength as shown in Fig. 4. A similar observation in another silicate phosphor, $Sr_2SiO_4:Eu^{2+}$, was reported by Park et al.[14] This phenomenon can be explained as follows. Qui et al. reported that the probability of energy transfer among Eu^{2+} ions increased when the Eu^{2+} concentration increased.[15] As the concentration of Eu^{2+} is increased, the distance between Eu^{2+} ions becomes short and the probability of energy transfer among Eu^{2+} ions increases. The probability of Eu^{2+} ions at higher levels of 5d which relax or make an energy transfer to the lower 5d levels of Eu^{2+} ions at the same or different sites increases with an increase of the Eu^{2+} concentration. Therefore, a shift of emission peak to a longer wavelength with an increase of Eu^{2+} concentration is possible.[14,15] However, because PL intensity drastically decreased when Eu^{2+} concentration was larger than 1 mol %,

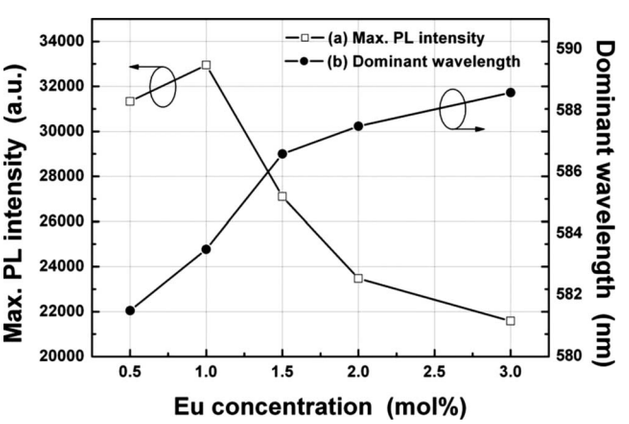

Figure 4. Maximum PL intensity and dominant wavelength of $Sr_3SiO_5:Eu^{2+}$ with various Eu^{2+} concentrations.

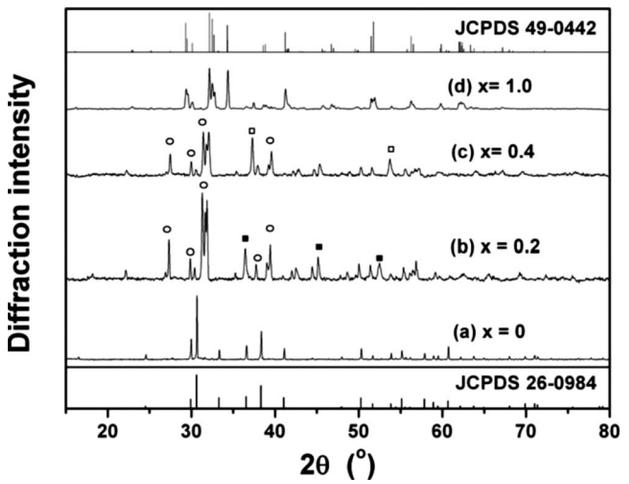

Figure 5. XRD patterns of $(Sr_{1-x}Ca_x)_3SiO_5:Eu^{2+}$ phosphor samples with various Ca content: (a) $x = 0$, (b) $x = 0.2$, (c) $x = 0.4$, and (d) $x = 1.0$; (○) Sr_2SiO_4 phase, (■) $CaSiO_3$ phase, and (□) CaO phase.

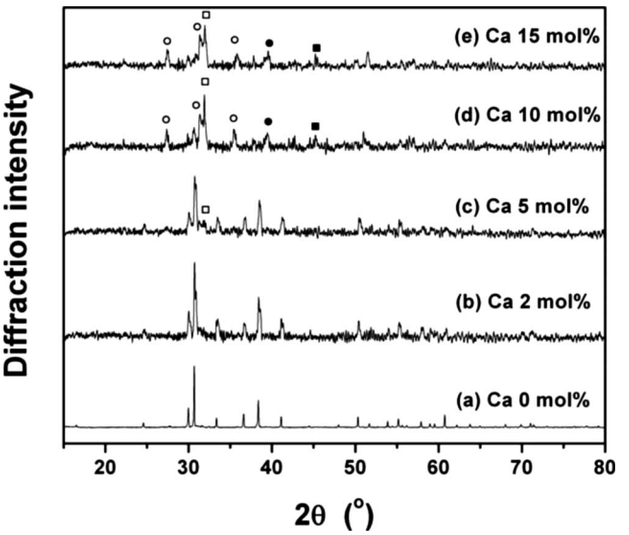

Figure 6. XRD patterns of $(Sr_{1-x}Ca_x)_3SiO_5:Eu^{2+}$ phosphor samples with various Ca content: (a) Ca 0 mol %, (b) Ca 2 mol %, (c) Ca 5 mol %, (d) Ca 10 mol %, and (e) Ca 15 mol %; (○) Sr_2SiO_4 phase, (■) $CaSiO_3$ phase, (●) Ca_2SiO_4 phase, and (□) Ca_3SiO_5 phase.

it seems inappropriate to control the PL band by increasing Eu^{2+} concentration. In the case of the 5d-4f transition of Ce^{3+} or Eu^{2+}, the emission band can be adjusted by a host modification such as cation substitution.[16-18] Thus, Sr^{2+} sites were substituted by Ca^{2+} or Ba^{2+} ions, because substitution of Sr^{2+} cation sites by other ions affects crystal field strength. It is believed that conspicuous variation of Eu^{2+} emission will be observed as the concentration of Ca^{2+} or Ba^{2+} increases in the host lattice, because the difference among effective ionic radii of Sr^{2+}, Ca^{2+}, and Ba^{2+} (Sr^{2+} = 1.18 Å, Ca^{2+} = 1.00 Å, and Ba^{2+} = 1.35 Å) is large.[19]

Figure 5 shows XRD patterns of $(Sr_{1-x}Ca_x)_3SiO_5:Eu^{2+}$ phosphors ($x = 0$, 0.2, 0.4, and 1.0). The structure of Ca_3SiO_5 is monoclinic (JCPDS card no. 49-0442), which is different from that of Sr_3SiO_5 (tetragonal structure) as shown in Fig. 5. Therefore, as Sr sites are substituted by Ca^{2+} ions, their crystal structure might change from tetragonal to monoclinic. In the case of Sr substitution by 20 or 40 mol % Ca, impurity phases such as Sr_2SiO_4, $CaSiO_3$, and CaO were observed. It is believed that the formation of single-phase $(Sr,Ca)_3SiO_5:Eu^{2+}$ is difficult due to the different crystal structures of Sr_3SiO_5 and Ca_3SiO_5; however, when Sr sites were fully substituted by Ca, a monoclinic Ca_3SiO_5 phase was formed. With increasing Ca substitution in the host, emission intensity of the phosphor severely decreased due to impurities and different crystal structures. When Ca ions totally replace Sr sites, orange-yellow emission was not observed under the excitation of blue light (450 nm). The PL spectrum is not included because the decrease of emission intensity is very severe without a band shift.

However, because the concentration of 20 mol % Ca might be too high to substitute Sr sites, $(Sr,Ca)_3SiO_5:Eu^{2+}$ with Ca concentrations less than 20 mol % were synthesized. The concentrations of Ca were as follows: 2, 5, 10, and 15 mol %. XRD patterns of the synthesized phosphor samples are depicted in Fig. 6. When the concentration of Ca was 2 mol %, there was very little impurity phase and the diffraction intensity of impurity phase was too weak to distinguish. As shown in Fig. 6, however, when the concentration of Ca was 5 mol %, an impurity phase appeared. The diffraction intensity of the impurity phase was much higher than that of Sr_3SiO_5 phase when the concentration of Ca was larger than 5 mol %. Therefore, in this experiment, the solubility limit of Ca into $Sr_3SiO_5:Eu^{2+}$ was revealed to be 5 mol %. However, for the 2 mol % of Ca substitution, conspicuous shift of the PL band was not observed due to the very low concentration of Ca substitution.

When Sr^{2+} sites were substituted by Ba^{2+} ions, the tetragonal phase was well maintained. Figure 7 shows powder XRD patterns of $(Sr_{1-x}Ba_x)_3SiO_5:Eu^{2+}$ phosphor samples. As the amount of Ba^{2+} ions was increased in the host lattice, the main diffraction peak of (202) shifted to lower angles, from 30.7° for $Sr_3SiO_5:Eu^{2+}$ to 29.2° for $Ba_3SiO_5:Eu^{2+}$. If there is a solubility limit, a continuous shift of the diffraction peak cannot be observed and each main (202) peak of Sr_3SiO_5 and Ba_3SiO_5 would appear at 30.7 and 29.2°, respectively. The change observed in the XRD patterns indicates that the Ba^{2+} ions substituted Sr^{2+} sites. As a result, the emission band of $(Sr_{1-x}Ba_x)_3SiO_5:Eu^{2+}$ was changed as shown in Fig. 8.

Figure 8 shows the PL spectra of $(Sr_{1-x}Ba_x)_3SiO_5:Eu^{2+}$ phosphor samples. When Ba^{2+} ions substituted Sr^{2+} sites at 20 mol %, the emission band shifted to a longer wavelength. Such a redshift can be explained by crystal field splitting. The Sr_3SiO_5 structure is built of Sr^{2+} ions, O^{2-} ions, and isolated SiO_4^{4-} tetrahedra. According to Glasser, all the O^{2-} ions are surrounded by regular octahedra of Sr^{2+}

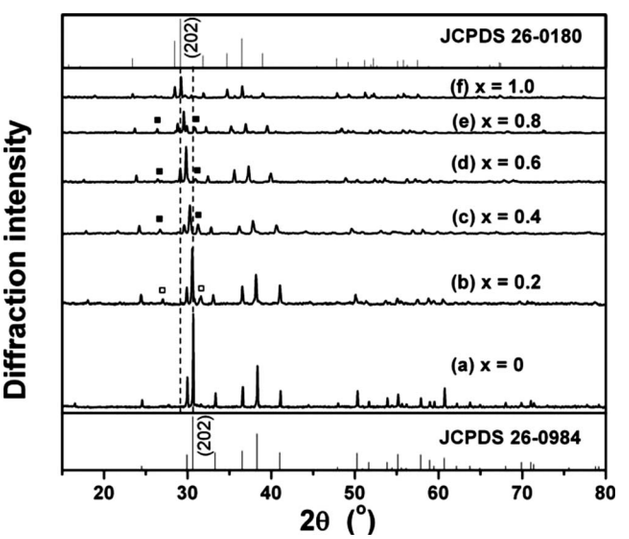

Figure 7. XRD patterns of $(Sr_{1-x}Ba_x)_3SiO_5:Eu^{2+}$ phosphor samples with various Ba content: (a) $x = 0$, (b) $x = 0.2$, (c) $x = 0.4$, (d) $x = 0.6$, (e) $x = 0.8$, and (f) $x = 1.0$; (□) Eu_2SiO_4 phase and (■) Ba_2SiO_4 phase.

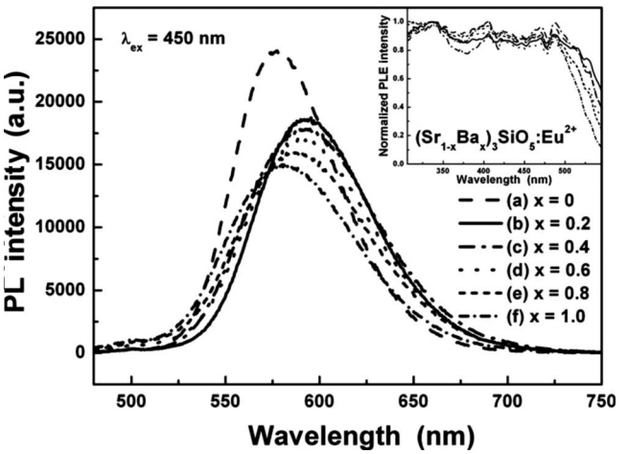

Figure 8. PL and normalized PLE spectra of $(Sr_{1-x}Ba_x)_3SiO_5:Eu^{2+}$ phosphor samples with various Ba content: (a) $x = 0$, (b) $x = 0.2$, (c) $x = 0.4$, (d) $x = 0.6$, (e) $x = 0.8$, and (f) $x = 1.0$.

ions in which there are Sr^{2+} ions at the corners surrounding central O^{2-} ions.[20] The octahedra all have one fourfold axis parallel to *c*, and they share corners. Each Sr^{2+} ion is bonded to two oxygen atoms, and these two oxygen atoms have only one Sr^{2+} ion. The coordination of the Sr^{2+} ion is completed with oxygen atoms which belong to SiO_4^{4-} tetrahedra. It was confirmed by Park et al. that the octahedral symmetry around the Sr^{2+} ion is lowered as Sr^{2+} sites are substituted by Ba^{2+}.[21] Due to the lowered symmetry, the crystal field splitting of the 5d band of Eu^{2+} increases so that the emission band of Eu^{2+} shifts to a longer wavelength. The crystal field splitting (Δ) can be calculated using PLE spectra,[10] and the values of Δ of the phosphors were calculated from the PLE data shown in the Fig. 8 inset. The calculated values of Δ of $(Sr_{1-x}Ba_x)_3SiO_5:Eu^{2+}$ are as follows: 8707, 9140, 9186, 9296, 9319, and 9364 cm^{-1} ($x = 0$, 0.2, 0.4, 0.6, 0.8, and 1.0, respectively). The increase of Δ of the 5d band of Eu^{2+} ions means that the crystal field surrounding Eu^{2+} gets stronger as the Ba concentration is increased. Therefore, from the PLE spectra it could be confirmed that the crystal field splitting of the 5d band of Eu^{2+} ions increased as the amount of Ba increased in the Sr_3SiO_5 host. Although the value of Δ of the 5d band of Eu^{2+} ions was shown to increase with increasing Ba concentration, the PLE and PL bands showed blueshifts when the concentration of Ba exceeded 20 mol %. The blueshift of the PLE and PL bands could be explained by a higher $4f^6d^1$ band position due to the Nephelauxetic effect with increasing Ba concentration in the host lattice. The electronegativity of Ba (0.89) is lower than that of Sr (0.95).[22] The difference of electronegativity between cation and anion increases, and hence the covalency of the host lattice decreases as the concentration of Ba^{2+} increases. That is, the covalent nature decreases, which causes a blueshift of the emission of Eu^{2+} according to the Nephelauxetic effect. Figure 9 shows the schematic diagram for the effects of crystal field and covalency (Nephelauxetic effect) on the energy level of a Eu^{2+} ion. In this system, the Nephelauxetic effect and the crystal field effect are in competition when Ba replaces Sr^{2+} sites. As the concentration of Ba increases in the host, covalency decreases and the position of the $4f^65d^1$ level of Eu^{2+} increases, while crystal field splitting increases. When the concentration of Ba^{2+} is below 20 mol %, the emission band is shifted to a longer wavelength. From this result, it is certain that the effect of crystal field is larger than that of covalency by Ba^{2+} substitution at 20 mol %. However, when the concentration of Ba^{2+} exceeded 20 mol %, the emission band of Eu^{2+} returned to a shorter wavelength (blueshift). This result implies that the covalency factor is more dominant compared to crystal field splitting when Ba^{2+} content is over 20 mol %. In Fig. 7, the powder XRD patterns show impurity peaks with very small diffraction intensity. Although the emission intensity of Eu^{2+} may be decreased slightly due to small amount of impurity phase, the impurity phases with the exception of Sr_3SiO_5 and Ba_3SiO_5 have no effect on the emission band shift of orange-yellow emission band of Eu^{2+}. The fact that the impurity phase of Ba_2SiO_4 has a green emission band is well known in the literature.[23] Therefore, one can conclude that the emission band change is purely due to the correlated effect of crystal field and covalency.

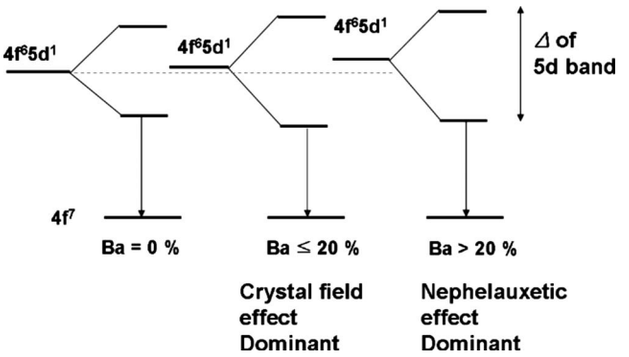

Figure 9. Schematic diagram of energy band change of Eu^{2+} in $(Sr_{1-x}Ba_x)_3SiO_5:Eu^{2+}$ phosphors. (Δ represents the crystal field splitting of the 5d level of the Eu^{2+} ion.)

Figure 10 shows the CIE color chromaticity diagram. The CIE color coordinates of $Sr_3SiO_5:Eu^{2+}$ and YAG:Ce phosphors are (0.537, 0.451) and (0.447, 0.535), respectively. The line connecting color coordinates of a blue LED and those of a YAG:Ce phosphor passes through the white region on the CIE chromaticity diagram. However, the line connecting color coordinates of a blue LED and those of a $Sr_3SiO_5:Eu^{2+}$ phosphor does not pass through the white region on the CIE chromaticity diagram. Therefore, when the orange-yellow-emitting $Sr_3SiO_5:Eu^{2+}$ phosphor is used to fabricate white LEDs using commercial blue LEDs, it is difficult to obtain natural daylight-like white light. Hence, it is necessary to modify the emission band of $Sr_3SiO_5:Eu^{2+}$ and/or add another phosphor to the $Sr_3SiO_5:Eu^{2+}$. Although Sr^{2+} sites were substituted by Ca^{2+} or Ba^{2+}, green spectral intensity was not enhanced. Therefore, it seems to be

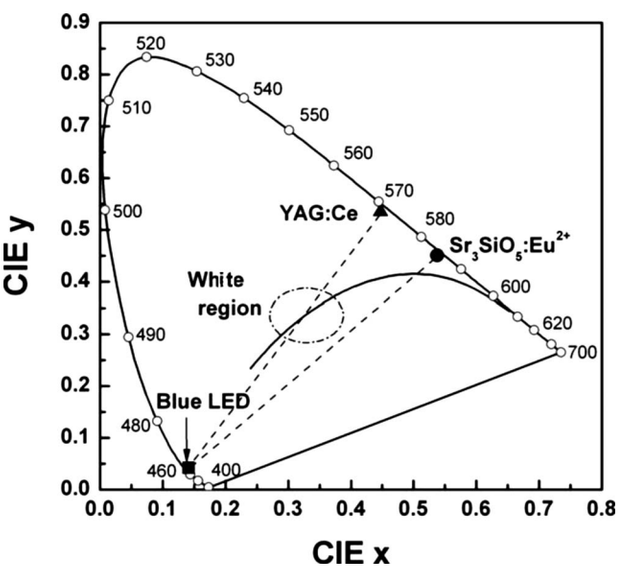

Figure 10. The CIE color coordinates of $Sr_3SiO_5:Eu^{2+}$ (●), YAG:Ce (▲), and blue LED (■).

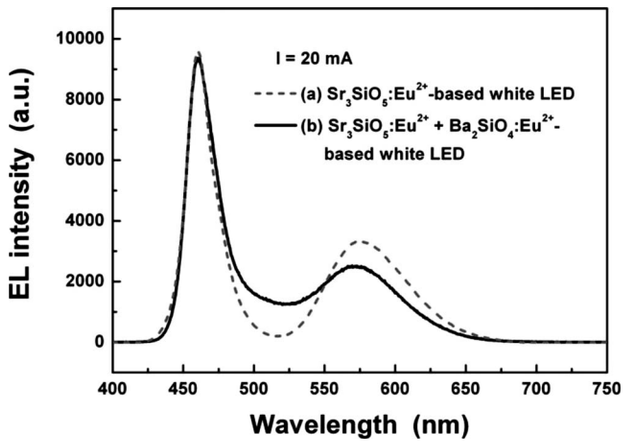

Figure 11. EL spectra of blue LED-pumped white LEDs using (a) $Sr_3SiO_5:Eu^{2+}$ and (b) two-phosphor mixture of $Sr_3SiO_5:Eu^{2+}$ and $Ba_2SiO_4:Eu^{2+}$.

appropriate to add a green-emitting phosphor to $Sr_3SiO_5:Eu^{2+}$ in order to make the color coordinates of blue LED-pumped white LEDs closer to those of daylight-like white light.

Figure 11 shows the spectra of blue LED-pumped white LEDs. Blue LED-pumped white LEDs were fabricated using either $Sr_3SiO_5:Eu^{2+}$ or a two-phosphor mixture ($Sr_3SiO_5:Eu^{2+}$ and a green-emitting $Ba_{1.98}SiO_4:Eu^{2+}_{0.02}$ phosphor). [A green-emitting $Ba_{1.98}SiO_5:Eu^{2+}_{0.02}$ ($Ba_2SiO_4:Eu^{2+}$) phosphor was synthesized by solid-state reaction method in this study.] In the case of the white LED using the two-phosphor mixture, the green emission was stronger than that of the white LED using $Sr_3SiO_5:Eu^{2+}$. The CIE color coordinates of white LEDs using $Sr_3SiO_5:Eu^{2+}$ and the two-phosphor mixture were (0.343, 0.281) and (0.349, 0.339), respectively. The CIE color coordinates of the latter were closer to the point of the daylight-like white light in the chromaticity diagram than that of the former.

Further investigation has been carried out to evaluate whether $Sr_3SiO_5:Eu^{2+}$ could be applicable to n-UV LED-pumped white LEDs, and n-UV LED-pumped white LEDs have also been fabricated with $Sr_3SiO_5:Eu^{2+}$ and a green-emitting $Ba_2SiO_4:Eu^{2+}$ phosphor. Figure 12 shows the EL spectrum of the white LED. The EL spectrum of the n-UV LED-pumped white LED consists of three emission bands which are attributed to the n-UV LED, $Ba_2SiO_4:Eu^{2+}$, and $Sr_3SiO_5:Eu^{2+}$, respectively. The n-UV LED-pumped $Sr_3SiO_5:Eu^{2+}$-based white LED showed warm white light. This is due to weak eye sensitivity for the blue light in the region of 400–410 nm and strong orange-yellow intensity. $Sr_3SiO_5:Eu^{2+}$ absorbed n-UV light from the n-UV LED and then emitted strong orange-yellow light. This result confirms that $Sr_3SiO_5:Eu^{2+}$ is a good candidate for n-UV LED-pumped white LEDs.

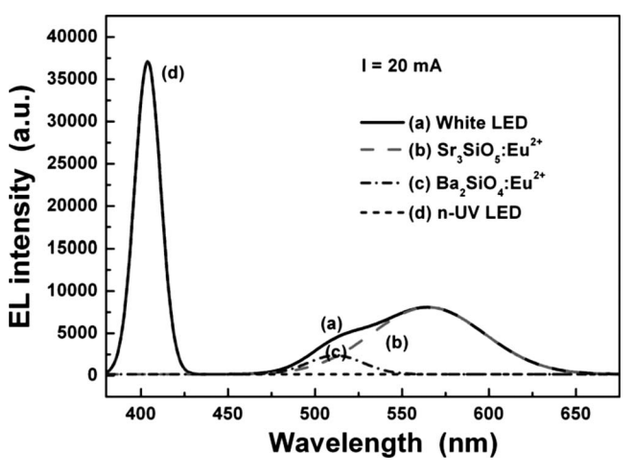

Figure 12. EL spectrum of n-UV LED-pumped white LED by using a two-phosphor mixture of $Sr_3SiO_5:Eu^{2+}$ and $Ba_2SiO_4:Eu^{2+}$.

Conclusion

$Sr_3SiO_5:Eu^{2+}$ showed a strong orange-yellow emission under blue and n-UV light excitation. When the concentration of Eu^{2+} ions was increased in the host lattice, the emission band of $Sr_3SiO_5:Eu^{2+}$ shifted slightly to a longer wavelength due to energy transfer between Eu^{2+} ions. When Sr^{2+} sites were substituted by Ba^{2+}, the Eu^{2+} emission band shifted to a longer wavelength initially and then returned to a shorter wavelength. The change in emission band was explained based on crystal field and covalency effects (Nephelauxetic effect). The substitution of Sr ions by Ba ions induces the two effects on the band shift simultaneously. It is believed that the crystal field effect is dominant when Ba concentration is smaller than 20 mol %, and the Nephelauxetic effect is dominant when Ba concentration is larger than 20 mol %. When a green-emitting $Ba_2SiO_4:Eu^{2+}$ phosphor was blended with $Sr_3SiO_5:Eu^{2+}$, the fabricated white LED showed good CIE color coordinates close to natural white. An n-UV LED-based white LED fabricated with $Ba_2SiO_4:Eu^{2+}$ and $Sr_3SiO_5:Eu^{2+}$ showed three well-resolved emission bands. That means $Sr_3SiO_5:Eu^{2+}$ is also a promising candidate for application to n-UV LED-pumped white LEDs.

Acknowledgment

This work was supported by the Center for Electronic Packaging Materials (ERC) of MOST/KOSEF.

Korea Advanced Institute of Science and Technology assisted in meeting the publication costs of this article.

References

1. S. Nakamura and G. Fasol, *The Blue Laser Diode: GaN Based Light Emitters and Lasers*, Springer, Berlin (1997).
2. S. Lee and S. Y. Seo, *J. Electrochem. Soc.*, **149**, J85 (2002).
3. H. S. Jang, H. Yang, S. W. Kim, J. Y. Han, S.-G. Lee, and D. Y. Jeon, *Adv. Mater. (Weinheim, Ger.)*, **20**, 2696 (2008).
4. Y.-H. Won, H. S. Jang, W. B. Im, J. S. Lee, and D. Y. Jeon, *Appl. Phys. Lett.*, **89**, 231909 (2006).
5. R.-J. Xie, N. Hirosaki, N. Kimura, K. Sakuma, and M. Mitomo, *Appl. Phys. Lett.*, **90**, 191101 (2007).
6. R.-J. Xie, N. Hirosaki, M. Mitomo, K. Takahashi, and K. Sakuma, *Appl. Phys. Lett.*, **88**, 101104 (2006).
7. H. S. Jang and D. Y. Jeon, *Opt. Lett.*, **32**, 3444 (2007).
8. Y.-H. Won, H. S. Jang, W. B. Im, and D. Y. Jeon, *J. Electrochem. Soc.*, **155**, J226 (2008).
9. H. S. Jang, J. H. Kang, Y.-H. Won, K.-M. Chu, and D. Y. Jeon, *Opt. Lett.*, **33**, 2140 (2008).
10. J. K. Park, C. H. Kim, S. H. Park, H. D. Park, and S. Y. Choi, *Appl. Phys. Lett.*, **84**, 1647 (2004).
11. G. Blasse and B. C. Grabmaier, *Luminescent Materials*, Springer, Berlin (1994).
12. G. Blasse, *J. Solid State Chem.*, **62**, 207 (1986).
13. R.-J. Xie, N. Hirosaki, M. Mitomo, K. Sakuma, and N. Kimura, *Appl. Phys. Lett.*, **89**, 241103 (2006).
14. J. K. Park, M. A. Lim, C. H. Kim, H. D. Park, J. T. Park, and S. Y. Choi, *Appl. Phys. Lett.*, **82**, 683 (2003).
15. J. Qiu, K. Miura, N. Sugimoto, and K. Hirao, *J. Non-Cryst. Solids*, **213-214**, 266 (1997).
16. J. S. Yoo, S. H. Kim, W. T. Yoo, G. Y. Hong, K. P. Kim, J. Rowland, and P. H. Holloway, *J. Electrochem. Soc.*, **152**, G382 (2005).
17. J. S. Kim, Y. H. Park, J. C. Choi, and H. L. Park, *J. Electrochem. Soc.*, **152**, H135 (2005).
18. H. S. Jang, W. B. Im, D. C. Lee, D. Y. Jeon, and S. S. Kim, *J. Lumin.*, **126**, 371 (2007).
19. *CRC Handbook of Chemistry and Physics*, 84th ed., D. R. Lide, Editor, CRC Press, Boca Raton, FL (2003).
20. L. S. D. Glasser, *Acta Crystallogr.*, **18**, 455 (1965).
21. J. K. Park, K. J. Choi, J. H. Yeon, S. J. Lee, and C. H. Kim, *Appl. Phys. Lett.*, **88**, 043511 (2006).
22. L. Pauling, *The Nature of the Chemical Bond*, 3rd ed., Cornell University Press, Ithaca, NY (1960).
23. S. H. M. Poort, W. Janssen, and G. Blasse, *J. Alloys Compd.*, **260**, 93 (1997).